ELSEVIER

Journal of Computational and Applied Mathematics 109 (1999) 41–63

JOURNAL OF COMPUTATIONAL AND APPLIED MATHEMATICS

www.elsevier.nl/locate/cam

Numerical solution of the expanding stellar atmosphere problem

Peter H. Hauschildt[a,*], E. Baron[b]

[a] *Department of Physics and Astronomy & Center for Simulational Physics, University of Georgia, Athens, GA 30602-2451, USA*

[b] *Department of Physics and Astronomy, University of Oklahoma, 440 W. Brooks, Rm 131, Norman, OK 73019-0225, USA*

Received 10 February 1998; received in revised form 16 August 1998

Abstract

In this paper we discuss numerical methods and algorithms for the solution of NLTE stellar atmosphere problems involving expanding atmospheres, e.g., found in novae, supernovae and stellar winds. We show how a scheme of nested iterations can be used to reduce the high dimension of the problem to a number of problems with smaller dimensions. As examples of these sub-problems, we discuss the numerical solution of the radiative transfer equation for relativistically expanding media with spherical symmetry, the solution of the multi-level nonLTE statistical equilibrium problem for extremely large model atoms, and our temperature correction procedure. Although modern iteration schemes are very efficient, parallel algorithms are essential in making large-scale calculations feasible, therefore we discuss some parallelization schemes that we have developed. © 1999 Elsevier Science B.V. All rights reserved.

Keywords: Stellar atmospheres; Radiative transfer; Parallel numerical algorithms; NLTE

1. Introduction

Astronomy is sometimes described as a "passive science" since it depends on observations of distant objects, rather than on laboratory experiments. Due to both laboratory measurements of important astrophysical atomic and nuclear data, and advances in computational power which allow us to perform "numerical experiments" that situation has changed in the last 50 years, and astronomy has matured into the modern subject of astrophysics. Still, our ability to understand the nature of astronomical objects is hampered by the fact that astronomical observations detect radiation that has been emitted primarily from the surface of objects. Thus in order to determine the structure of stellar

* Corresponding author.

E-mail address: yeti@hal.physast.uga.edu (P.H. Hauschildt)

0377-0427/99/$ - see front matter © 1999 Elsevier Science B.V. All rights reserved.
PII: S0377-0427(99)00153-3

objects one must solve the radiation transport equation and compare "synthetic spectra" with observations. The numerical solution of the radiation transport problems is an important prerequisite for the calculation of model stellar atmospheres. The simulated spectrum is then compared to observed spectra of objects such as stars, where the radiation is mostly emitted from the outer layers. In the case of very low mass stars and brown dwarfs, the atmosphere is also crucial in determining the interior structure of these objects since it serves as a boundary condition for the equations of stellar structure in a nearly fully convective "star".

Additionally, in objects such as supernovae, where the the explosion causes the "atmosphere" (here used to paraphrase "the region where the spectrum forms") to expand rapidly, a time series of spectra reveal the entire structure of the object as the ejected material expands and thins and the atmosphere moves inward in the material. In the case of expanding objects such as hot stars (many with strong stellar winds), novae, and supernovae; the radiation transport equation must be solved simultaneously with the hydrodynamical equations, an even more difficult computational problem than static stars. We focus here on the computation of model atmospheres and the numerical solution of the radiation transport equation in expanding media with known velocity fields. This is a frequently encountered situation, e.g., when the hydrodynamic behavior is known a priori, or can be calculated separately from the radiation transport by using a nested iteration scheme. The feedback between detailed synthetic spectrum calculations and hydrodynamic simulations is often the primary tool for testing a specific hydrodynamical model.

Our group has developed the very general nonLTE (NLTE) stellar atmosphere computer code `PHOENIX` [1,4,5,11–15,17] which can handle very large model atoms as well as line blanketing by hundreds of millions of atomic and molecular lines. This code is designed to be both portable and very flexible: it is used to compute model atmospheres and synthetic spectra for, e.g., novae, supernovae, M and brown dwarfs, O to M giants, white dwarfs and accretion disks in Active Galactic Nuclei (AGN). The radiative transfer in `PHOENIX` is solved in spherical geometry and includes the effects of special relativity (including advection and aberration) in the modeling. The `PHOENIX` code allows us to include a large number of NLTE and LTE background spectral lines and solves the radiative transfer equation for each of them *without* using simple approximations like the Sobolev approximation. Therefore, the profiles of spectral lines must be resolved in the co-moving (Lagrangian) frame. This requires many wavelength points (we typically use 150,000 to 300,000 points). Since the CPU time scales linearly with the number of wavelength points, the CPU time requirements of such calculations are large. In addition, (NLTE) radiative rates for both line and continuum transitions must be calculated and stored at every spatial grid point for each transition, which requires large amounts of storage and can cause significant performance degradation if the corresponding routines are not optimally coded.

In strict LTE the radiation and matter are assumed to be in equilibrium with each other everywhere throughout the atmosphere. In LTE the source function is assumed to be given by the Planck function (see below). In NLTE, the radiation is no longer assumed to be in equilibrium with the matter and hence the full coupling between matter and radiation must be calculated in order to calculate the source function.

We concentrate here on the calculation of model atmospheres for expanding media and, in addition, describe some of the important parts of the numerous numerical algorithms used in `PHOENIX`: the numerical solution of the radiation transport equation, the nonLTE rate equations, and the

parallelization of the code. An important problem in these calculations is to find a consistent solution of the very diverse equations that describe the various physical processes. We have developed a scheme of nested iterations that enables us to separate many of the variables (e.g., separating the temperature correction procedure from the calculation of the NLTE occupation numbers). This allows us to compute far more detailed stellar atmosphere models than was previously possible. We will give an outline of these methods in this paper.

In order to take advantage of the enormous computing power and vast aggregate memory sizes of modern parallel supercomputers, both potentially allowing much faster model construction as well as more sophisticated models, we have developed a parallel version of PHOENIX. Since the code uses a modular design, we have implemented different parallelization strategies for different modules (e.g., radiative transfer, NLTE rates, atomic and molecular line opacities) in order to maximize the total parallel speed-up of the code. In addition, our implementation allows us to change the distribution of computational work onto different nodes both via input files and dynamically during a model run, which gives a high degree of flexibility to optimize performance for both a number of different parallel supercomputers (we are currently using IBM SP2s, SGI Origin 2000s, HP/Convex SPP-2000s, and Cray T3Es) and for different model parameters. Since PHOENIX has both large CPU and memory requirements we have developed the parallel version of the code using a MIMD approach. We use the MPI message passing library [22] for portability and *simultaneously* use both task and data parallelism in order to optimize the parallel speed-up [4,14].

2. The problem

2.1. Overview

Our goal (for the purposes of this paper) is to construct self-consistent models of expanding stellar atmospheres. The atmosphere itself is parameterized by a number of parameters, e.g., the total energy emitted by the object (luminosity L), the mass M of the star, the abundances of the elements (in some cases as function of the location in the atmosphere). This means that we have to find a set of physical variables such as temperatures, densities, population number of each atomic energy level and the radiation field, at *each* location in the atmosphere so that all constraint equations are simultaneously fulfilled. In Fig. 1 we show this requirement in a simplified graphical form where the arrows indicate *direct* (usually nonlinear) coupling between the different blocks. The number of variables that need to be addressed is, formally, very large. A typical case of a spherically symmetric shell model with 50 radial points requires a set of 50 temperatures and gas pressures (or matter densities). In addition to this we include a set of about 6000 individual energy levels for atoms and ions directly, the population of each must be known at every radial point, adding a total of 300,000 variables. In order to calculate the population numbers, we need a description of the radiation field at each radial point and on a set of wavelength points (the rates that govern the transitions between atomic energy levels are integrals of the mean intensity of the radiation field over wavelength). We typically need 100,000 to 300,000 wavelength point to describe the complete radiation field, which adds, in the worst case, 15 million variables to the system.

Fortunately, most of these formal variables are tightly coupled to a much smaller set of variables which we might, therefore, consider the "fundamental" variables of the model atmosphere problem.

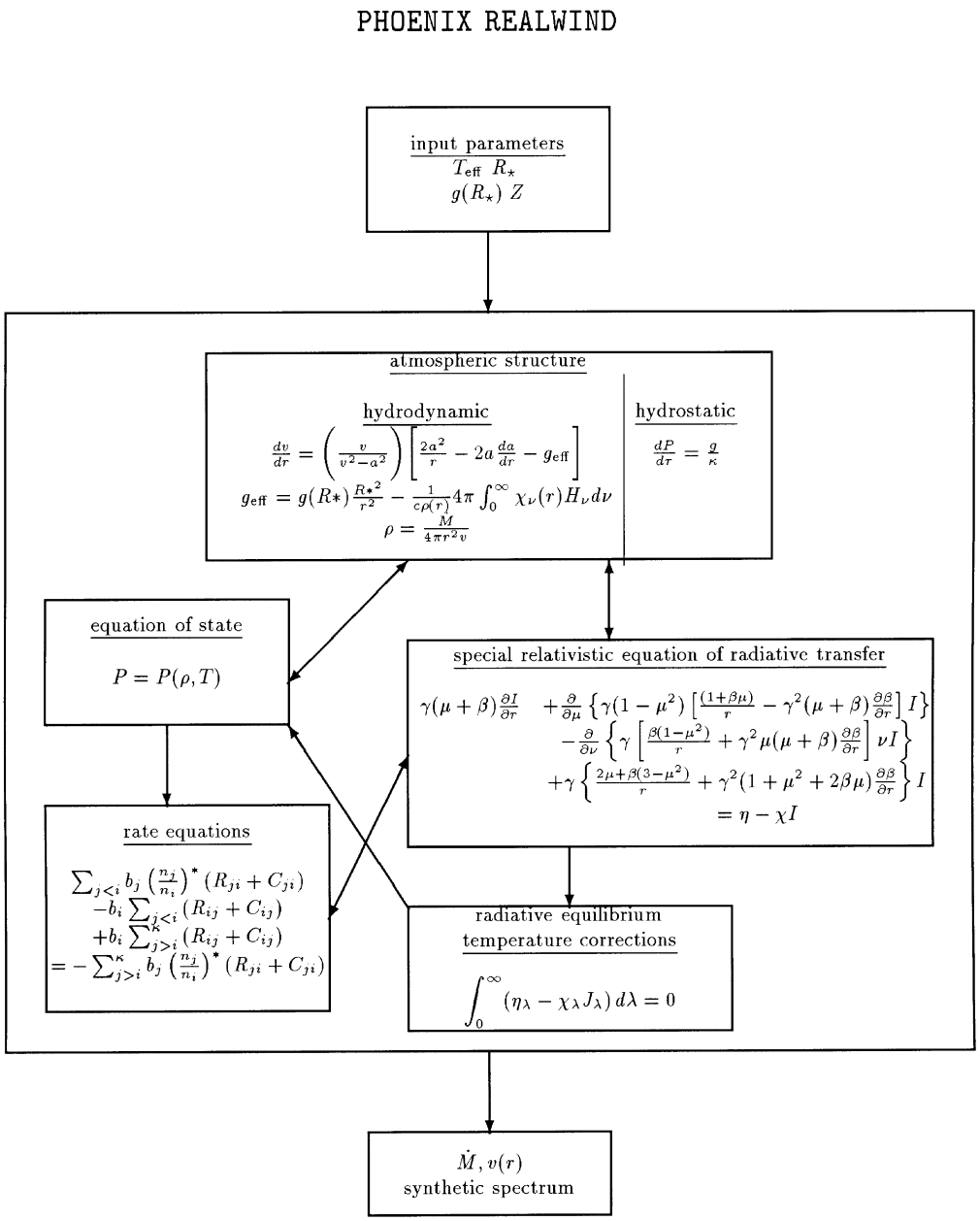

Fig. 1. Relation between (some of) the physical and mathematical blocks that describe the physics of a stellar atmosphere. In order to calculate a model atmosphere, a set of value of the physical variables, e.g., temperatures, densities, population densities and the radiation field, must be found that satisfies all constraints simultaneously.

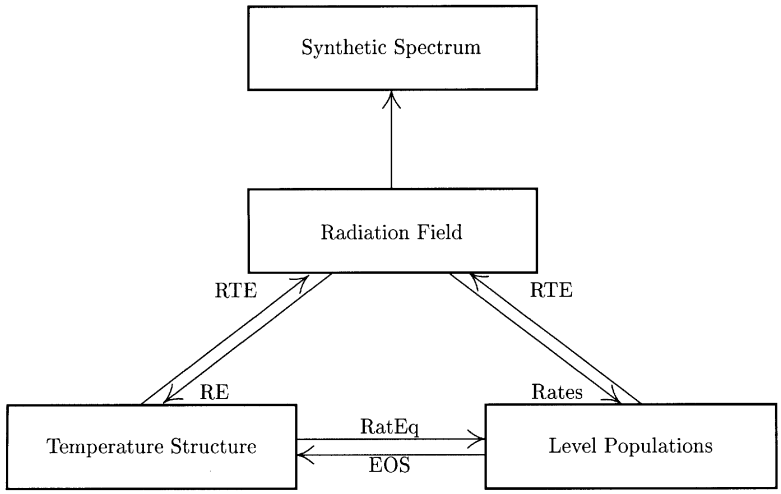

- **RTE: Radiative Transfer Equation**
- **RE: Radiative Equilibrium**
- **EOS: (generalized) Equation Of State**
- **RatEq: Rate Equations**
- **Rates: radiative & collisional rates**

Fig. 2. Relations between the main types of variables represented by blocks are indicated. The labels name the equations that relate the block to each other.

In our approach, these fundamental variables are the temperatures T, the gas pressures $P_{\rm gas}$, and the population numbers n_i at each radial point r_i. The radiation field is considered a "derived" quantity and the problem is thus reduced to find a set of physical variables $\{T, P_{\rm gas}, n_i\}$ at each radial point i so that the system outlined in Fig. 2 is self-consistent. With this approach we have reduced the number of variables from several million to a few hundred thousand, which is still a daunting number.

Although it is possible to analytically bring the system into a form so that it could be solved by a Newton–Raphson approach [24], this idea is computationally prohibitive because of its enormous memory and time requirements (however, for smaller systems this approach has been used successfully). Furthermore, this approach is complex to implement and it is relatively hard to add more "physics" to the model atmosphere. We have thus developed a scheme of nested iterative solutions that considers the direct (or strong) couplings between important variables directly and iteratively accounts for the indirect coupling between sets of variables. With this approach the problem of constructing the model atmosphere can be separated into solving a large number of smaller problems with only a few 100 variables. The global requirement of a self-consistent solution is then reach by iteratively coupling these sets of variables to each other until a prescribed accuracy has been reached. This method works because the level of coupling between the variables is very different. For example, the temperature structure of the atmosphere depends mostly on the global constraint of energy conservation (represented by wavelength integrals over the whole spectrum) and on the *ratios* of several averaged opacities, but it does not depend strongly on the fine *details* of the radiation

field or the *individual* population of the vast majority of the atomic levels. Therefore, *correction* to the temperature structure can be calculated approximately. The current errors of, e.g., the energy conservation equations, must be calculated exactly in order to this scheme to function, however, this is relatively simple. The general idea of calculating errors exactly but corrections to the variables approximately will work if the approximations are good enough for the scheme to converge at all. This method will require more iterations to reach convergence but this is more than offset by faster individual iterations and (very often) by better robustness. The latter is very important if many model atmospheres have to be constructed or if no good initial guesses for the variables are known.

In the following sections we will concentrate on a few key parts of the expanding atmosphere problem: the numerical solution of the radiative transfer equation for a single wavelength point (this will deliver the radiation field for a given set of variables at every wavelength), the solution of the NLTE statistical equilibrium equations (coupling the radiation field to the level populations), and an outline of the temperature correction procedure. The latter is important because it allows us to solve the NLTE statistical equilibrium equations separately for individual elements (and even ionization stages), which dramatically reduces the dimension of the sub-problems that have to be solved within the global nested iteration scheme. In this paper we will not discuss problems related to the hydrodynamics of the expanding medium or the details of the equation of state calculations, both of which are important topics.

2.2. Radiative transfer in expanding media

The equation of radiative transfer (RTE) in spherical symmetry for moving media has been solved with a number of different methods, e.g. Monte Carlo calculations [2,7,21], Sobolev methods [8], the tangent ray method [26], and the DOME method [19]. Only the tangent ray and the DOME method have been used to solve the RTE for very fast expanding shells (e.g. supernovae or novae) including the necessary special relativistic terms. Both methods need relatively large amounts of CPU time to compute the radiation field, mainly because of the need for matrix inversions (tangent ray method) or matrix diagonalization (DOME), which make both of them impractical for use within radiation-hydrodynamic studies of nova or supernova explosions. It has been shown [16] that the special relativistic terms in the RTE can be very important, even in the optically thick regions of expanding shells, and lead to results different than from the simpler approach which simply neglects the relativistic terms.

Recently, iterative methods for the solution of the RTE have been developed, based on the philosophy of operator perturbation [6,32]. Following these ideas, different approximate Λ-operators for this "accelerated Λ-iteration" (ALI) method have been used successfully [10,29,36] and have been applied to the construction of nonLTE, radiative equilibrium models of stellar atmospheres [36].

We describe the use of the short-characteristic method [29,30] to obtain the formal solution of the special relativistic, spherically symmetric radiative transfer equation (SSRTE) along its characteristic rays and then use a band-diagonal approximation to the discretized Λ-operator [11,18,30] as our choice of the approximate Λ-operator. This method can be implemented very efficiently to obtain an accurate solution of the SSRTE for continuum and line transfer problems using only modest amounts of computer resources.

The co-moving frame radiative transfer equation for spherically symmetric flows can be written as [27]

$$\gamma(1+\beta\mu)\frac{\partial I_\nu}{\partial t}+\gamma(\mu+\beta)\frac{\partial I_\nu}{\partial r}+\frac{\partial}{\partial\mu}\left\{\gamma(1-\mu^2)\left[\frac{1+\beta\mu}{r}-\gamma^2(\mu+\beta)\frac{\partial\beta}{\partial r}-\gamma^2(1+\beta\mu)\frac{\partial\beta}{\partial t}\right]I_\nu\right\}$$
$$-\frac{\partial}{\partial\nu}\left\{\gamma\nu\left[\frac{\beta(1-\mu^2)}{r}+\gamma^2\mu(\mu+\beta)\frac{\partial\beta}{\partial r}+\gamma^2\mu(1+\beta\mu)\frac{\partial\beta}{\partial t}\right]I_\nu\right\}$$
$$+\gamma\left\{\frac{2\mu+\beta(3-\mu^2)}{r}+\gamma^2(1+\mu^2+2\beta\mu)\frac{\partial\beta}{\partial r}+\gamma^2[2\mu+\beta(1+\mu^2)]\frac{\partial\beta}{\partial t}\right\}I_\nu$$
$$=\eta_\nu-\chi_\nu I_\nu. \tag{1}$$

$\beta=v/c$ is the velocity in units of the speed of light, c; and $\gamma=(1-\beta^2)^{-1/2}$ is the usual Lorentz factor. Equation (1) is a integro-differential equation, since the emissivity η_ν contains J_ν, the zeroth angular moment of I_ν:

$$\eta_\nu=\kappa_\nu S_\nu+\sigma_\nu J_\nu+\sum_{\text{lines}}\sigma_l(\nu)\int\phi_l J_\nu\,\mathrm{d}\nu$$

with

$$J_\nu=\frac{1}{2}\int_{-1}^{1}\mathrm{d}\mu\, I_\nu, \tag{2}$$

where S_ν is the source function, κ_ν is the absorption coefficient, σ_ν is the scattering coefficient for continuum processes, σ_l are the line scattering coefficients, and ϕ_l is the line profile function. The independent variables are the radius r of the shell, the cosine μ of the angle between the radial direction and the propagation vector of the light (with $\mu=-1,1$ for radially inward and outward moving light, respectively), and the frequency $\nu=c/\lambda$ for a wavelength λ of the light. With the assumption of time-independence, $\partial I_\nu/\partial t=0$, and a monotonic velocity field Eq. (1) becomes a boundary-value problem in the spatial coordinate and an initial value problem in the frequency or wavelength coordinate.

Switching from frequency to wavelength (Eq. (1) is presented in Ref. [11] in wavelength), the mean intensity J_λ is obtained from the source function S_λ by a formal solution of the RTE which is symbolically written using the Λ-operator Λ_λ as

$$J_\lambda=\Lambda_\lambda S_\lambda. \tag{3}$$

In the case of the transition of a two-level atom, we have

$$\bar{J}=\Lambda S, \tag{4}$$

where $\bar{J}=\int\phi(\lambda)J_\lambda\,\mathrm{d}\lambda$, $\Lambda=\int\phi(\lambda)\Lambda_\lambda\,\mathrm{d}\lambda$ with the normalized line profile $\phi(\lambda)$. The line source function, for the simple case of a two-level atom without continuum and background absorption or scattering, is given by $S=(1-\varepsilon)\bar{J}+\varepsilon B$, where ε denotes the thermal coupling parameter and B is Planck's function.

The Λ-iteration method, i.e. to solve Eq. (4) by a fixed-point iteration scheme of the form

$$\bar{J}_{\text{new}}=\Lambda S_{\text{old}},\qquad S_{\text{new}}=(1-\varepsilon)\bar{J}_{\text{new}}+\varepsilon B, \tag{5}$$

fails in the case of large optical depths and small ε. This result is caused by the fact that the largest eigenvalue of the amplification matrix (in the case of Doppler profiles) is approximately [26] $\lambda_{\max} \approx (1-\varepsilon)(1-T^{-1})$, where T is the optical thickness of the medium. For small ε and large T, this is very close to unity and, therefore, the convergence rate of the Λ-iteration is very poor. A physical description of this effect can be found in Mihalas [25].

2.2.1. The operator splitting method

The idea of the ALI or operator splitting method is to reduce the eigenvalues of the amplification matrix in the iteration scheme [6] by introducing an approximate Λ-operator (ALO) Λ^* and to split Λ according to

$$\Lambda = \Lambda^* + (\Lambda - \Lambda^*) \tag{6}$$

and rewrite Eq. (4) as

$$\bar{J}_{\text{new}} = \Lambda^* S_{\text{new}} + (\Lambda - \Lambda^*) S_{\text{old}}. \tag{7}$$

This relation can be written as [22]

$$[1 - \Lambda^*(1-\varepsilon)]\bar{J}_{\text{new}} = \bar{J}_{\text{fs}} - \Lambda^*(1-\varepsilon)\bar{J}_{\text{old}}, \tag{8}$$

where $\bar{J}_{\text{fs}} = \Lambda S_{\text{old}}$. Eq. (8) is solved to get the new values of $\bar{J}$ which is then used to compute the new source function for the next iteration cycle.

Mathematically, the ALI method belongs to the same family of iterative methods as the Jacobi or the Gauss–Seidel methods [9]. These methods have the general form

$$Mx^{k+1} = Nx^k + b \tag{9}$$

for the iterative solution of a linear system $Ax = b$ where the system matrix A is split according to $A = M - N$. In the case of the ALI method we have $M = 1 - \Lambda^*(1-\varepsilon)$ and, accordingly, $N = (\Lambda - \Lambda^*)(1-\varepsilon)$ for the system matrix $A = 1 - \Lambda(1-\varepsilon)$. The convergence of the iterations depends on the spectral radius, $\rho(G)$, of the iteration matrix $G = M^{-1}N$. For convergence the condition $\rho(G) < 1$ must be fulfilled, this puts a restriction on the choice of Λ^*. In general, the iterations will converge faster for a smaller spectral radius. To achieve a significant improvement compared to the Λ-iteration, the operator Λ^* is constructed so that the eigenvalues of the iteration matrix G are much smaller than unity, resulting in swift convergence. Using parts of the exact Λ matrix (e.g., its diagonal or a tri-diagonal form) will optimally reduce the eigenvalues of the G. The calculation and the structure of Λ^* should be simple in order to make the construction of the linear system in Eq. (8) fast. For example, the choice $\Lambda^* = \Lambda$ is best in view of the convergence rate (it is equivalent to a direct solution by matrix inversion) but the explicit construction of Λ is more time consuming than the construction of a simpler Λ^*. The solution of the system Eq. (8) in terms of linear algebra, using modern linear algebra packages such as, e.g., `LAPACK`, is so fast that its CPU time can be neglected for the small number of variables encountered in 1D problems (typically the number of discrete shells is about 50). However, for 2D or 3D problems the size of Λ gets very large due to the much larger number of grid points as compared to the 1D case. Matrix inversions, which are necessary to solve Eq. (8) directly, therefore become extremely time consuming. This makes the direct solution of Eq. (8) more CPU intensive even for Λ^*'s of moderate bandwidth, except for the trivial case of a diagonal Λ^*. Different methods like modified conjugate gradient methods [33] may be effective for these 2D or 3D problems.

The CPU time required for the solution of the RTE using the ALI method depends on several factors: (a) the time required for a formal solution and the computation of $\bar{J}_{\rm fs}$, (b) the time needed to construct Λ^*, (c) the time required for the solution of Eq. (8), and (d) the number of iterations required for convergence to the prescribed accuracy. Points (a)–(c) depend mostly on the number of discrete shells, and can be assumed to be fixed for any given configuration. However, the number of iterations required to convergence depends strongly on the bandwidth of Λ^*. This indicates, that there is an *optimum bandwidth* of the Λ^*-operator which will result in the shortest possible CPU time needed for the solution of the RTE, which we will discuss below.

2.2.2. Computation of Λ^*

The formal solution of the SSRTE is performed along the characteristic rays on a mesh $\{r_i\}$, $i = 1,\ldots,N_{\rm s}$ of discrete shells using the short-characteristic (SC) method of Olson and Kunasz [30] with piece-wise parabolic or linear interpolation. The characteristic rays are *curved* in the case of the SSRTE and have to be calculated before the solution of the radiative transfer equation proceeds (see [11] for details). Improvements in this method [11,18] include an improved angle integration using generalized Simpson quadrature and a generalization of the approximate Λ-operator to an arbitrary number of bands below and above the main diagonal (up to the full Λ-operator).

We describe here the general procedure of calculating the Λ^* with *arbitrary* bandwidth, up to the full Λ-operator, for the SC method in spherical symmetry [25]. Although we consider the SSRTE as given in the previous section, the same procedure applies for radiative transfer problems in static media or in (static or moving) media with plane-parallel symmetry. The specialization of the formulae given in this section is straightforward.

The formal solution along a characteristic of the SSRTE (hereafter, a "ray") is done using a polynomial interpolation of the source function, S, along the ray. For reasons of numerical stability, we use linear or quadratic interpolation of S along each ray, although this is not required by the method. This leads to the following expressions for the specific intensity $I(\tau_i)$ along a ray (cf. Ref. [30] for a derivation of the formulae):

$$I^k(\tau_i^k) = I^k(\tau_{i-1}^k)\exp(\tau_{i-1}^k - \tau_i^k) + \int_{\tau_{i-1}^k}^{\tau_i^k} \hat{S}(\tau)\exp(\tau_{i-1}^k - \tau)\,{\rm d}\tau, \tag{10}$$

$$I_i^k \equiv I_{i-1}^k \exp(-\Delta\tau_{i-1}^k) + \Delta I_i^k,$$

where the superscript k labels the ray; τ_i^k denotes the optical depth along the ray k with $\tau_1^k \equiv 0$ and $\tau_{i-1}^k \leqslant \tau_i^k$ while τ^k is calculated, e.g., using piecewise linear interpolation of $\hat{\chi}$ along the ray, viz.

$$\Delta\tau_{i-1}^k = (\hat{\chi}_{i-1} + \hat{\chi}_i)|s_{i-1}^k - s_i^k|/2 \tag{11}$$

and

$$\Delta I_i^k = \alpha_i^k \hat{S}_{i-1} + \beta_i^k \hat{S}_i + \gamma_i^k \hat{S}_{i+1}, \tag{12}$$

where i is the "running" index along the ray and $|s_{i-1}^k - s_i^k|$ is the geometrical path length between points i and $i-1$. The expressions for the coefficients α_i^k, β_i^k and γ_i^k are given in Ref. [30] (see also Ref. [11]).

We describe the construction of Λ^* for arbitrary bandwidth using the example of a characteristic that is tangential to an arbitrary shell: Ray k is the ray that is tangent to shell $k+1$. The intersection

points (including the point of tangency) are labeled from left to right, the direction in which the formal solution proceeds. Ray k has $2k+1$ points of intersection with discrete shells $1 \ldots k+1$. To compute row j of the discrete Λ-operator (or Λ-matrix), Λ_{ij}, we sequentially label the intersection points of the ray k with the shell i, and define auxiliary quantities λ_{ij}^k and $\hat{\lambda}_{ij}^k$ as follows:

$$\begin{aligned}
&\lambda_{i,j}^k = 0 \quad \text{for } i < j-1,\\
&\lambda_{j-1,j}^k = \gamma_{j-1}^k \quad \text{for } i = j-1,\\
&\lambda_{j,j}^k = \lambda_{j-1,j}^k \exp(-\Delta\tau_{j-1}^k) + \beta_j^k \quad \text{for } i = j,\\
&\lambda_{j+1,j}^k = \lambda_{j,j}^k \exp(-\Delta\tau_j^k) + \alpha_{j+1}^k \quad \text{for } i = j+1,\\
&\lambda_{i,j}^k = \lambda_{i-1,j}^k \exp(-\Delta\tau_{i-1}^k) \quad \text{for } j+1 < i \leqslant k+1.
\end{aligned} \tag{13}$$

For the calculation of $\hat{\lambda}_{i,j}^k$, we obtain

$$\begin{aligned}
&\hat{\lambda}_{i,j}^k = \lambda_{i-1,j}^k \exp(-\Delta\tau_{i-1}^k) \quad \text{for } i = k+2,\\
&\hat{\lambda}_{i,j}^k = \hat{\lambda}_{i-1,j}^k \exp(-\Delta\tau_{i-1}^k) \quad \text{for } k+2 < i < k+j+2,\\
&\hat{\lambda}_{i,j}^k = \hat{\lambda}_{i-1,j}^k \exp(-\Delta\tau_{i-1}^k) + \alpha_i^k \quad \text{for } i = k+j+2,\\
&\hat{\lambda}_{i,j}^k = \hat{\lambda}_{i-1,j}^k \exp(-\Delta\tau_{i-1}^k) + \beta_i \quad \text{for } i = k+j+3,\\
&\hat{\lambda}_{i,j}^k = \hat{\lambda}_{i-1,j}^k \exp(-\Delta\tau_{i-1}^k) + \gamma_i^k \quad \text{for } i = k+j+4,\\
&\hat{\lambda}_{i,j}^k = \hat{\lambda}_{i-1,j}^k \exp(-\Delta\tau_{i-1}^k) \quad \text{for } k+j+5 \leqslant i \leqslant 2k+1.
\end{aligned} \tag{14}$$

Using the λ_{ij}^k and λ_{ij}^k, we can now write the Λ-Matrix as

$$\Lambda_{ij} = \sum_k \left(\sum_{\{l\}} w_{l,j}^k \lambda_{l,j}^k + \sum_{\{l'\}} w_{2(k+1)-l',j}^k \hat{\lambda}_{2(k+1)-l',j}^k \right), \tag{15}$$

where $w_{i,j}^k$ are the angular quadrature weights, $\{l\}$ is the set $\{i \leqslant k+1\}$ and $\{l'\}$ is the set $\{i > k+1\}$. This expression gives the *full* Λ-matrix, it can easily be specialized to compute only *certain bands* of the Λ-matrix. In that case, not all of the $\lambda_{i,j}^k$ and $\hat{\lambda}_{i,j}^k$ have to be computed, reducing the CPU time from that required for the computation of the full Λ-matrix.

2.2.3. Numerical considerations

The calculation of Λ^* using the algorithm outlined can be vectorized and parallelized with respect to the ray index k and the row index j for any given bandwidth of Λ^*. In addition, quantities like $\exp(-\Delta\tau_{i-1}^k)$, α_i^k, β_i^k and γ_i^k can be pre-calculated and stored, a process which is fully vectorizable and parallelizable.

For each point on a ray, the computation of the specific intensity uses about seven floating point operations (flops), whereas the computation of the $\lambda_{i,j}^k$ and $\hat{\lambda}_{i,j}^k$ takes only 1 flop *per intersection point*. In addition, about three flops are needed for the integration over the angle coordinate μ in order to compute the mean intensities J and the Λ^*-operator. We have to calculate the formal solution for $N_{\mathrm{T}}(N_{\mathrm{T}}+1) + N_{\mathrm{T}} + 2N_{\mathrm{S}}N_{\mathrm{C}}$ points, where N_{S} is the number of discrete shells, N_{C} is the number of core intersecting characteristics and $N_{\mathrm{T}} = N_{\mathrm{S}} - 1$ is the number of tangent rays.

Therefore, the number of flops required for the computation of the specific intensities at all points is $\approx 10[(N_S+1)(N_S-1)+2N_SN_C]$. To estimate the number of flops required for the calculation of a Λ^*-operator with a bandwidth of $N_B \leqslant N_S$, we assume that each point of a ray has N_B nearest neighbors, thus *overestimating* the number of operations. In this approximation, we have to compute $\leqslant N_B N_T(N_T+2)+2N_BN_SN_C$ auxiliary variables $\lambda^k_{i,j}$ or $\hat{\lambda}^k_{i,j}$. Therefore, about $\leqslant 4N_B[(N_S-1)(N_S+1)+2N_SN_C]$ floating-point operations are needed to compute the Λ^*-operator and the ratio of the numerical work needed for the computation of a Λ^*-operator with a bandwidth of N_B and one formal solution is of the order of $2N_B/5$. This expression actually *significantly* overestimates the number of operations required for the construction of the Λ^* operator, in particular for larger bandwidths (the effects of the boundaries become more important for larger bandwidths). For example, according to this estimate the computation of the full Λ-matrix for $N_S = 50$ takes about the same time as 20 formal solutions, however, the actual time used for the construction of the full Λ-matrix corresponds only to about 6 formal solutions on many machines. This indicates that the number of iterations must be rather small in order to make ALOs with small bandwidth competitive in terms of speed for the solution of radiative transfer problems and that the initial guess for the source function will have a large influence on the optimum bandwidth. The best strategy is to use monitoring to predict the "optimum" bandwidth that gives the shortest time for the solution of the SSRTE at any given wavelength point in an "adaptive bandwidth operator splitting" method, see Ref. [18] for details and results for a number of machines.

In order to accelerate convergence the Ng method [28] or the Orthomin method [35] may be used (see Auer [3] for a review of different acceleration methods). These methods can cut down the number of iterations required to reach a prescribed accuracy by a factor of two or more with only a small increase in computational overhead.

2.3. NLTE calculations

In order to solve Eq. (1), the emissivity η_λ must be known, but η_λ depends on the NLTE level populations and therefore the NLTE rate equations must be solved simultaneously with Eq. (1). This is further complicated by the fact that the NLTE rate equations depend on the radiation field itself. The NLTE rate equations have the form [24]

$$\sum_{j<i} n_j(R_{ji}+C_{ji}) - n_i\left\{\sum_{j<i}\left(\frac{n_j^*}{n_i^*}\right)(R_{ij}+C_{ji}) + \sum_{j>i}(R_{ij}+C_{ij})\right\} + \sum_{j>i} n_j\left(\frac{n_i^*}{n_j^*}\right)(R_{ji}+C_{ij}) = 0. \tag{16}$$

In Eq. (16), n_i is the actual, nonLTE population density of a level i and the symbol n_i^* denotes the so-called LTE population density of the level i, which is given by

$$n_i^* = \frac{g_i}{g_\kappa} n_\kappa \frac{2h^3 n_e}{(2\pi m)^{3/2}(kT)^{3/2}} \exp\left(-\frac{E_i - E_\kappa}{kT}\right). \tag{17}$$

Here n_κ denotes the *actual*, i.e., nonLTE, population density of the ground state of the next higher ionization stage of the same element; g_i and g_κ are the statistical weights of the levels i and κ, respectively. In Eq. (17), E_i is the excitation energy of the level i and E_κ denotes the ionization energy from the ground state to the corresponding ground state of the next higher ionization stage.

The actual, nonLTE electron density is given by n_e. The system of rate equations is closed by the conservation equations for the nuclei and the charge conservation equation (cf. Ref. [24]).

The sums in Eq. (16) extend only over the levels that are included in our model atoms; for example, in singly ionized iron our model atom consists of 675 energy levels [13]. The weaker radiative transitions are treated as LTE background opacity (see Refs. [12,13]).

The rate coefficients for radiative and collisional transitions between two levels i and j (including transitions from and to the continuum, see below) are given by R_{ij} and C_{ij}, respectively. In our notation, the upward (absorption) radiative rate coefficients R_{ij} $(i < j)$ are given by

$$R_{ij} = \frac{4\pi}{hc} \int_0^\infty \alpha_{ij}(\lambda) J_\lambda(\lambda) \lambda \, \mathrm{d}\lambda, \tag{18}$$

whereas the downward (emission) radiative rate coefficients R_{ji} $(i < j)$ are given by

$$R_{ji} = \frac{4\pi}{hc} \int_0^\infty \alpha_{ji}(\lambda) \left(\frac{2hc^2}{\lambda^5} + J_\lambda(\lambda) \right) \exp\left(-\frac{hc}{k\lambda T} \right) \lambda \, \mathrm{d}\lambda. \tag{19}$$

Here, J is the mean intensity, T the electron temperature, h and c are Planck's constant and the speed of light, respectively. For the purposes of this paper, we assume that cross section $\alpha_{ij}(\lambda)$ of the transition $i \to j$ at the wavelength λ is known for both line and continuum transitions and that it is the same for both absorption and emission processes (complete redistribution).

Not all atomic processes fit neatly into the above scheme where the rates are in detailed balance. Nonthermal ionization by fast electrons, K-capture, Auger emission, and two-photon decay are important in various stages of the evolution of novae and supernovae. They can be included in the above formulation with reasonable approximations, however.

2.3.1. The rate operator

As described above, a simple fixed-point iteration scheme for the solution of the rate equations will converge much too slowly to be useful for most cases of practical interest. Therefore, we use an extension of the operator splitting idea for the solution of the rate equations.

We rewrite the rate equations in the form of an "operator equation." This equation is then used to introduce an "approximate rate operator" in analogy to the approximate Λ-operator which can then be used to iteratively solve the rate and statistical equations by an operator splitting method, details of the approach are given in [12].

We introduce first the "rate operator" $[R_{ij}]$ for upward transitions in analogy to the Λ-operator. $[R_{ij}]$ is defined so that

$$R_{ij} = [R_{ij}][n]. \tag{20}$$

Here, $[n]$ denotes the "population density operator", which can be considered as the vector of the population densities of all levels at all points in the medium under consideration. The radiative rates are (linear) functions of the mean intensity J, which is given by $J(\lambda) = \Lambda(\lambda) S(\lambda)$, where $S = \eta(\lambda)/\chi(\lambda)$ is the source function. Using the Λ-operator, we can write $[R_{ij}][n]$ as

$$[R_{ij}][n] = \frac{4\pi}{hc} \int \alpha_{ij}(\lambda) \Lambda(\lambda) S(\lambda) \lambda \, \mathrm{d}\lambda. \tag{21}$$

This can be brought into the form (see [12] for details)

$$[R_{ij}][n] = \frac{4\pi}{hc}\left[\int_0^\infty \alpha_{ij}(\lambda)\Psi(\lambda)E(\lambda)\lambda\,\mathrm{d}\lambda\right][n]. \tag{22}$$

The corresponding expression for the emission rate-operator $[R_{ji}]$ is given by

$$[R_{ji}][n] = \frac{4\pi}{hc}\int_0^\infty \alpha_{ji}(\lambda)\left\{\frac{2hc^2}{\lambda^5} + \Psi(\lambda)[E(\lambda)][n]\right\}\exp\left(-\frac{hc}{k\lambda T}\right)\lambda\,\mathrm{d}\lambda, \tag{23}$$

where we have used the definition

$$\Lambda(\lambda) = \Psi(\lambda)/\chi(\lambda) \tag{24}$$

and $[E(\lambda)]$ is a *linear* operator such that $[E(\lambda)][n]$ gives the emissivity $\eta(\lambda)$.

Using the rate operator, we can write the rate equations in the form

$$\sum_{j<i} n_j([R_{ji}][n] + C_{ji}) - n_i\left\{\sum_{j<i}\left(\frac{n_j^*}{n_i^*}\right)([R_{ij}][n] + C_{ji}) + \sum_{j>i}([R_{ij}][n] + C_{ij})\right\}$$

$$+\sum_{j>i} n_j\left(\frac{n_i^*}{n_j^*}\right)([R_{ji}][n] + C_{ij}) = 0. \tag{25}$$

This form shows, explicitly, the nonlinearity of the rate equations with respect to the population densities. Note that in addition, the rate equations are nonlinear with respect to the electron density via the collisional rates. Furthermore, the charge conservation constraint condition directly couples the electron densities and the population densities of all level of all atoms and ions with each other.

In analogy to the operator splitting method discusses above, we split the rate operator, by writing $[R_{ij}] = [R_{ij}^*] + ([R_{ij}] - [R_{ij}^*]) \equiv [R_{ij}^*] + [\Delta R_{ij}]$ (analog for the downward radiative rates), where $[R_{ij}^*]$ is the "approximate rate-operator". We then rewrite the rate R_{ij} as

$$R_{ij} = [R_{ij}^*][n_{\mathrm{new}}] + [\Delta R_{ij}][n_{\mathrm{old}}] \tag{26}$$

and analogously for the downward radiative rates. In Eq. (26), $[n_{\mathrm{old}}]$ denotes the current (old) population densities, whereas $[n_{\mathrm{new}}]$ are the updated (new) population densities to be calculated. The $[R_{ij}^*]$ and $[R_{ji}^*]$ are linear functions of the population density operator $[n_k]$ of any level k, due to the linearity of η and the usage of the Ψ-operator instead of the Λ-operator.

If we insert Eq. (26) into Eq. (16), we obtain the following system for the new population densities:

$$\sum_{j<i} n_{j,\mathrm{new}}[R_{ji}^*][n_{\mathrm{new}}] - n_{i,\mathrm{new}}\left\{\sum_{j<i}\left(\frac{n_j^*}{n_i^*}\right)[R_{ij}^*][n_{\mathrm{new}}] + \sum_{j>i}[R_{ij}^*][n_{\mathrm{new}}]\right\}$$

$$+\sum_{j>i} n_{j,\mathrm{new}}\left(\frac{n_i^*}{n_j^*}\right)[R_{ji}^*][n_{\mathrm{new}}] + \sum_{j<i} n_{j,\mathrm{new}}([\Delta R_{ji}][n_{\mathrm{old}}] + C_{ji})$$

$$-n_{i,\mathrm{new}}\left\{\sum_{j<i}\left(\frac{n_j^*}{n_i^*}\right)([\Delta R_{ij}][n_{\mathrm{old}}]+C_{ji})+\sum_{j>i}([\Delta R_{ij}][n_{\mathrm{old}}]+C_{ij})\right\}$$

$$+\sum_{j>i}n_{j,\mathrm{new}}\left(\frac{n_i^*}{n_j^*}\right)([\Delta R_{ji}][n_{\mathrm{old}}]+C_{ij})=0. \tag{27}$$

Due to its construction, the $[R_{ij}^*]$-operator contains information about the influence of a particular level on *all* radiative transitions. Therefore, we are able to treat the complete multi-level nonLTE radiative transfer problem including active continua and overlapping lines. The $[E(\lambda)]$-operator, at the same time, gives us information about the strength of the coupling of a radiative transition to all levels that are considered. This information may be used to include or neglect certain couplings *dynamically* during the iterative solution of Eq. (27). Furthermore, we have not yet specified either a method for the formal solution of the radiative transfer equation or a method for the construction of the approximate Λ-operator (and, correspondingly, the $[R_{ij}^*]$-operator). We proceed by considering rapidly expanding spherically symmetric media and use the tri-diagonal ALO given by Hauschildt [11]. However, any method for the formal solution of the radiative transfer equation and the construction of the ALO may be used, including multi-dimensional and/or time dependent methods.

2.3.2. Solution of the statistical equations

The system Eq. (27) for $[n_{\mathrm{new}}]$ is nonlinear with respect to the $n_{i,\mathrm{new}}$ and n_{e} because the coefficients of the $[R_{ij}^*]$ and $[R_{ji}^*]$-operators are quadratic in $n_{i,\mathrm{new}}$ and the dependence of the Saha–Boltzmann factors and the collisional rates on the electron density, respectively. The system is closed by the abundance and charge conservation equations. To simplify the iteration scheme, and to take advantage of the fact that not all levels strongly influence all radiative transitions, we use a linearized and splitted iteration scheme for the solution of Eq. (27). This scheme has the further advantage that many different elements in different ionization stages and even molecules can be treated consistently. A problem where this is important is the modeling of nova and supernova atmospheres, where there are typically very large temperature gradients within the line forming region of the atmosphere.

To linearize Eq. (27), we follow [31] and replace terms of the form $n_{j,\mathrm{new}}[R_{ji}^*][n_{\mathrm{new}}]$ in Eq. (27) by $n_{j,\mathrm{old}}[R_{ji}^*][n_{\mathrm{new}}]$

$$\sum_{j<i}n_{j,\mathrm{old}}[R_{ji}^*][n_{\mathrm{new}}]-n_{i,\mathrm{old}}\left\{\sum_{j<i}\left(\frac{n_j^*}{n_i^*}\right)[R_{ij}^*][n_{\mathrm{new}}]+\sum_{j>i}[R_{ij}^*][n_{\mathrm{new}}]\right\}$$

$$+\sum_{j>i}n_{j,\mathrm{old}}\left(\frac{n_i^*}{n_j^*}\right)[R_{ji}^*][n_{\mathrm{new}}]+\sum_{j<i}n_{j,\mathrm{new}}([\Delta R_{ji}][n_{\mathrm{old}}]+C_{ji}) \tag{28}$$

$$-n_{i,\mathrm{new}}\left\{\sum_{j<i}\left(\frac{n_j^*}{n_i^*}\right)([\Delta R_{ij}][n_{\mathrm{old}}]+C_{ji})+\sum_{j>i}([\Delta R_{ij}][n_{\mathrm{old}}]+C_{ij})\right\}$$

$$+\sum_{j>i}n_{j,\mathrm{new}}\left(\frac{n_i^*}{n_j^*}\right)([\Delta R_{ji}][n_{\mathrm{old}}]+C_{ij})=0. \tag{29}$$

This removes the major part of the nonlinearity of Eq. (27) but the modified system is still nonlinear with respect to n_e and still has the high dimensionality of the original system. However, as has been noted before, not all levels are strongly coupled to all other levels. Eq. (29) can be solved for each element (or groups of elements if they are coupled tightly) *separately* if the electron density is given. Therefore, we split the electron density calculation from the rate equation solution so that the n_e can be considered as given during the rate equation solution process and changes in the electron density are then accounted for in an outer iteration to find a consistent solution of the rate equations and the electron densities.

The most important advantage of this method is that it requires the solution of large *linear* systems and low-dimensional nonlinear system (for the electron density). Thus, its solution is more stable and uses much less computer resources (time and memory) than the direct solution of the original nonlinear equations. This allows us to treat many more levels with this method then with more conventional algorithms. Using a nested iteration scheme like the one described here will slow down the convergence of the iterations, but this is more than offset for by the possibility of calculating much larger models with less memory. Since we are able to solve a separate equation for each group of elements, we can trivially parallelize the solution by distributing the groups among the available processors. Convergence acceleration methods can in principle be used, but they frequently lead to convergence instabilities in the nested iterations for the solution of the statistical equilibrium equations.

We have so far assumed that the electron density n_e is given. Although this is a good assumption if only trace elements are considered, the electron density may be sensitive to nonLTE effects. This can be taken into account by using either a fixed point iteration scheme for the electron density or, if many species or molecules are included in the nonLTE equation of state, by a modification of the LTE partition functions to include the effects of nonLTE in the ionization equilibrium. The latter method replaces the partition function, $Q = \sum g_i \exp(-E_i/kT)$, with its nonLTE generalization, $Q_{\mathrm{NLTE}} = \sum b_i g_i \exp(-E_i/kT)$, and uses Q_{NLTE} in the solution of the ionization/dissociation equilibrium equation. We use this method because of the large number of elements with various ionization stages as well as molecules and condensation of dust grains included in statistical equilibrium calculations (and not all of them in nonLTE).

Our iteration scheme for the solution of the multi-level nonLTE problem can be summarized as follows: (1) for given n_i and n_e, solve the radiative transfer equation at each wavelength point and update the radiative rates and the approximate rate operator, (2) solve the linear system Eq. (29) for each group for a given electron density, (3) compute new electron densities (by either fixed point iteration or the generalized partition function method), (4) if the electron density has not converged to the prescribed accuracy, go back to step 2, otherwise go to step 1. The iterations are repeated until a prescribed accuracy for the n_e and the n_i is reached. It is important to account for coherent scattering processes during the solution of the wavelength dependent radiative transfer equation, it explicitly removes a global coupling from the iterations.

2.4. Temperature correction procedure

In the outermost level of the nested iteration scheme we also iterate for the temperature structure of the atmosphere using a generalization of the Unsöld–Lucy temperature correction scheme to spherical geometry and NLTE model calculations. This has proven to work very well even in extreme NLTE

cases such as nova and supernova atmospheres. The temperature correction procedure also requires virtually no memory and CPU time overheads. The Unsöld–Lucy correction scheme (see [23] for a discussion of this and other temperature correction schemes), uses the global constraint equation of energy conservation to find corrections to the temperature that will fulfill energy conservation better than the previous temperatures. We have found it to be more stable than a Newton–Raphson linearization scheme and it allows us to separate the temperature corrections from the statistical equations discussed above.

To derive the Unsöld–Lucy correction, one uses the fact that the *ratios* of the wavelength-averaged absorption and extinction coefficients

$$\kappa_{\mathrm{P}} = \left(\int_0^\infty \kappa_\lambda B_l \, \mathrm{d}\lambda \right) \Big/ B, \tag{30}$$

$$\kappa_J = \left(\int_0^\infty \kappa_\lambda J_l \, \mathrm{d}\lambda \right) \Big/ J, \tag{31}$$

$$\chi_J = \left(\int_0^\infty \chi_\lambda F_l \, \mathrm{d}\lambda \right) \Big/ F \tag{32}$$

(where B, J, F denote the wavelength integrated Planck function, mean intensity and radiation flux, respectively) depend much less on values of the independent variables than do the averages themselves.

Dropping terms of order (v/c), one can then use the angular moments of the SSRTE to show that in order to obtain radiation equilibrium B should be corrected by an amount

$$\delta B(r) = \frac{1}{\kappa_{\mathrm{P}}} \{ \kappa_J J - \kappa_{\mathrm{P}} B + \dot{S}/(4\pi) \} - \left\{ 2(H(\tau = 0) - H_0(\tau = 0)) - \frac{1}{f q r^2} \int_r^R q r'^2 \chi_F (H(r') - H_0(r')) \, \mathrm{d}r' \right\}, \tag{33}$$

where $H \equiv F/4\pi$, $H_0(\tau)$ is the value of the target luminosity at that particular depth point (variable due to the velocity terms in the SSRTE and nonmechanical energy sources, the total *observed* luminosity $H_0(0)$ is an input parameter). Here, q is the "sphericity factor" given by

$$q = \frac{1}{r^2} \exp\left(\int_{r_{\mathrm{core}}}^r \frac{3f - 1}{r' f} \, \mathrm{d}r' \right),$$

where r_{core} is the inner radius of the atmosphere, R is the total radius, $f(\tau) = K(\tau)/J(\tau)$ is the "Eddington factor", and $K = \int \mu^2 I \, \mathrm{d}\mu$ is the second angular moment of the mean intensity. $\dot{S}$ describes all additional sources of energy such as mechanical energy supplied by winds or nonthermal ionization due to γ-ray deposition.

The first term in Eq. (33) corresponds simply to a Λ iteration term and will thus provide too small temperature corrections in the *inner* parts of the atmosphere (but work fine in the outer, optically thin parts). The second term of Eq. (33), however, is the dominant term in the inner parts of the atmosphere. It provides a very good approximation to the temperature corrections ΔT deep inside the atmosphere. Following [34], we found that it is sometimes better to modify this general scheme

by, e.g., excluding the contributions of extremely strong lines to the opacity averages used in the ΔT calculations because they tend to dominate the average opacity but do not contribute as much to the total error in the energy conservation constraint.

2.5. Global iteration scheme

As the first step in our outermost iteration loop (the "model iteration") we use the current best guess of $\{T, n_i\}$ as function of radius to solve the hydrostatic or hydrodynamic equations to calculate an improved run of $P_{\rm gas}$ with radius. Simultaneously, the population numbers are updated to account for changes in $P_{\rm gas}$. The next major step is the computation of the radiation field for each wavelength point (the "wavelength loop"), which has the prerequisite of a spectral line selection procedure for LTE background lines. Immediately after the radiation field at any given wavelength is known, the radiative rates and the rate operators are updated so that their calculation is finished after the last wavelength point. In the next steps, the population numbers are updated by solving the rate equations for each NLTE species and new electron densities are computed, this gives improved estimates for $\{n_i\}$. The last part of the model iteration is the temperature correction scheme outlined above (using opacity averages, etc. that were computed in the wavelength loop) which delivers an improved temperature structure. If the errors in the constraint equations are larger than a prescribed accuracy, the improved $\{T, n_i\}$ are used in another model iteration. Using this scheme, about 10–20 model iterations are typically required to reach convergence to better than about 1% relative errors, depending on the quality of the initial guess of the independent variables and the complexity of the model.

3. Parallelization

Solving the above set of coupled nonlinear equations for large numbers of NLTE species requires large amounts of memory to store the rates for each level in all the model atoms at each radial grid point, and large amounts of CPU time because many wavelength points are required in order to resolve the line profiles in the co-moving frame. In order to minimize both CPU and memory requirements we have parallelized the separate `Fortran 90` modules which make up the `PHOENIX` code. Our experience indicates that only the simultaneous use of data and task parallelism can deliver reasonable parallel speedups [14]. This involves:

(1) The radiative transfer calculation itself, where we divide up the characteristic rays among nodes and use a "reduce" operation to collect and send the J_ν to all the radiative transfer and NLTE rate computation tasks (data parallelism);

(2) the line opacity which requires the calculation of up to 50,000 Voigt profiles per wavelength point at each radial grid point, here we split the work amongst the processors both by radial grid points and by dividing up the individual lines to be calculated among the processors (combined data and task parallelism); and

(3) the NLTE calculations. The NLTE calculations involve three separate parts: the calculation of the NLTE opacities, the calculation of the rates at each wavelength point, and the solution of the NLTE rate and statistical equilibrium equations. To prevent communication overhead, each task computing the NLTE rates is forced to be on the same node with the corresponding

task computing NLTE opacities and emissivities, (combined data and task parallelism). The solution of the rate equations parallelizes trivially with the use of a diagonal approximate rate operator.

In the latest version of our code, PHOENIX 10.7, we have incorporated the additional strategy of distributing each NLTE species (the total number of ionization stages of a particular element treated in NLTE) on separate nodes. Since different species have different numbers of levels treated in NLTE (e.g. Fe II [singly ionized iron] has 617 NLTE levels, whereas H I has 30 levels), care is taken to balance the number of levels and NLTE transitions treated on each node to avoid unnecessary synchronization and communication problems. We have also parallelized the selection of background atomic and molecular LTE lines (a significant amount of work considering that our combined line lists currently include about 400 million lines and we expect line lists with about 1 billion lines in the near future). Although the line selection seems at first glance to be an inherently serial process, since a file sorted in wavelength with selected lines must be written to disk, we are able to obtain reasonable speedups, by employing a client–server model with a server line-selection task which receives the selected lines and writes them to disk and client nodes which read pieces (blocks) of the line list files and carry out the actual selection processes on each block of lines.

In addition to the combined data and task parallelism discussed above, PHOENIX also uses simultaneous explicit task parallelism by allocating different tasks (e.g., atomic line opacity, molecular line opacity, radiative transfer) to different nodes. This can result in further speed-up and better scalability but requires a careful analysis of the workload between different tasks (the workload is also a function of wavelength, e.g., different number of lines that overlap at each wavelength point) to obtain optimal load balancing.

3.1. Wavelength parallelization

The parallelization of the computational workload outlined in the previous paragraphs requires synchronization between the radiative transfer tasks and the NLTE tasks, since the radiation field and the Λ^* operator must be passed between them. In addition, our standard model calculations use 50 radial grid points and as the number of nodes increases, so too does the communication and loop overhead, therefore, pure data parallelism does not deliver good scalability. We found good speedup up to about five nodes for a typical calculation, with the speedup close to the theoretical maximum. However, for five nodes the communication and loop overheads begin to become significant and it is not economical to use more than 10 nodes (depending on the machine and the model calculation, it might be *necessary* to use more nodes to fit the data in the memory available on a single node).

Since the number of wavelength points in a calculation is very large and the CPU time scales linearly with the number of wavelength points, parallelization with respect to the wavelength points can lead to large speedups and to the ability to use very large numbers of nodes available on massively parallel supercomputers. This poses no difficulties for static configuration, but the coupling of the wavelengths points in expanding atmospheres makes the wavelength parallelization much more complex.

We have developed a wavelength parallelization based on a toroidal topology that uses the concept of wavelength "clusters" to distribute a set of wavelength points (for the solution of the

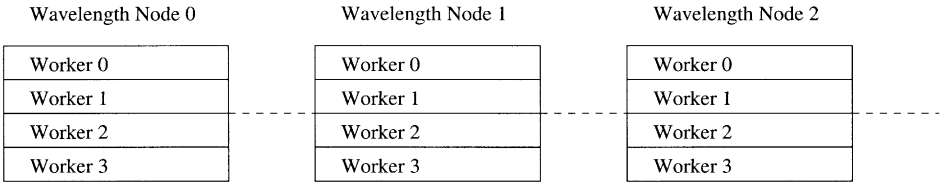

Fig. 3. The basic "torus" design of the wavelength-parallelized version of PHOENIX: groups of processors are divided up into wavelength clusters which will work on individual wavelength points, each wavelength cluster is further divided into a set of worker nodes, where each worker node is assigned a set of specific tasks, e.g., it will work on the LTE background line opacity for a set of radial points. Our design requires that each worker node on all wavelength clusters work on exactly the same set of tasks, although additional inherently serial operations can be assigned to one particular master worker, or master wavelength cluster. This reduces communication between clusters to its absolute minimum and allows the maximum speedup.

wavelength-dependent radiative transfer) onto a different set of nodes, see Fig. 3 [4]. In order to achieve optimal load balance and, more importantly, in order to minimize the memory requirements, each cluster (a column of nodes indicated in Fig. 3) works on a single wavelength point at any given time. Each cluster can consist of a *number* of "worker" nodes where the worker node group uses parallelization methods discussed above (see also Ref. [14]). In order to avoid communication overhead, we use *symmetric* wavelength clusters: each "row" of worker nodes in Fig. 3 performs identical tasks but on a different set of wavelength points for each cluster. We thus arrange the total number of nodes N in a rectangular matrix with n columns and m rows, where n is the number of clusters and m is the number of workers for each cluster, such that $N = n * m$. Another way of visualizing this parallelization technique is to consider each wavelength cluster as a single entity (although not a single node or CPU) that performs a variety of different tasks at each wavelength point. The entity (cluster) itself is then further subdivided into individual nodes or CPUs each of which perform a given set of tasks *at a particular wavelength point*. This topology can be implemented very efficiently in the context of the MPI library, see [14] for details.

For a static model atmosphere, all wavelengths and thus wavelength clusters are completely independent and execute in parallel with *no* immediate communication or synchronization along the rows of Fig. 3. Communication is only necessary *after* the calculation is complete for all wavelengths points on all nodes to collect, e.g., the rates and rate operators. Therefore, the speedup is close (80%) to the theoretical maximum, limited only by to combined IO bandwidth of the machine used.

In order to parallelize the spectrum calculations for a model atmosphere with a *global velocity field*, such as the expanding atmospheres of novae, supernovae or stellar winds, we need to take the mathematical character of the RTE into account. For monotonic velocity fields, the RTE is an initial value problem in wavelength (with the initial condition at the smallest wavelength for expanding atmospheres and at the largest wavelength for contracting atmospheres). This initial value problem must be discretized fully implicitly to ensure stability. In the simplest case of a first order discretization, the solution of the RTE for wavelength point i depends only on the results of the point $i-1$. In order to parallelize the spectrum calculations, the wavelength cluster n_i computing the

solution for wavelength point i must know the specific intensities from the cluster n_{i-1} computing the solution for point $i-1$. This suggests a "pipeline" solution to the wavelength parallelization, transforming the "matrix" arrangement of nodes into a "torus" arrangement where data are sent along the torus' circumference. Note that only the solution of the RTE is affected by this, the calculation of the opacities and rates remains independent between different wavelength clusters. In this case, the wavelength parallelization works as follows: Each cluster can independently compute the opacities and start the RT calculations (e.g., the Λ^* calculations, hereafter called the *pre-processing phase*), it then waits until it receives the specific intensities for the previous wavelength point, then it finishes the solution of the RTE and *immediately* sends the results to the wavelength cluster calculating the next wavelength point (to minimize waiting time, this is done with nonblocking send/receives), then proceeds to calculate the rates, etc. (hereafter called the *post-processing phase* and the new opacities for its *next* wavelength point and so on.

The important point in this scheme is that each wavelength cluster can execute the post-processing phase of its current wavelength point and pre-processing phase of its next wavelength point *independently and in parallel with all other clusters*. This means that the majority of the total computational work can be done in parallel, leading to a substantial reduction in wall-clock time per model. Ideal load balancing can be obtained by dynamically allocating wavelength points to wavelength clusters. This requires only primitive logic with no measurable overhead, however it requires also communication and an arbitration/synchronization process to avoid deadlocks. Typically, the number of clusters n (4–64) is much smaller than the number of wavelength points, $n_{\rm wl} \approx 300,000$, so that at any given time the work required for each wavelength point is roughly the same for each cluster (the work changes as the number of overlapping lines changes, for example). Therefore, a simple *round robin* allocation of wavelength points to clusters (cluster i calculates wavelength points i, $n+i$, $2n+i$ and so on) can be used which will result in nearly optimal performance if the condition $n \ll n_{\rm wl}$ is fulfilled. However, once the pipeline is full, adding further wavelength clusters cannot decrease the time required for the calculations, setting a limit for the efficient "radius" of the torus topology. However, this limit can be increased somewhat by increasing the number of worker nodes per wavelength cluster.

3.1.1. Scaling results

For a simple supernova test calculation, we examine both the scaling and performance tradeoff of spatial versus wavelength parallelization. Fig. 4 presents the results of our timing tests for one iteration of a Type Ic supernova model atmosphere, with a model temperature $T_{\rm model} = 12,000$ K (the observed luminosity is given by $L = 4\pi R^2 T_{\rm model}^4$), characteristic velocity $v_0 = 10,000$ km s^{-1}, 4666 NLTE levels, 163812 NLTE lines, 211680 LTE lines (for simplicity, all line profile were assumed to be Gaussian), nonhomogeneous abundances, and 260,630 wavelength points. This is a typical test for production calculations and we have designed this test to have the highest potential for synchronization, I/O waiting, and swapping to reduce performance to simulate a worst case scenario for the parallel performance. It is however, characteristic of the level of detail needed to accurately model supernovae. This calculation has also been designed to barely fit into the memory of a single node. The behavior of the speedup is very similar to the results obtained for test case using a model of a nova explosion [4]. The "saturation point" at which the wavelength pipeline fills and no further speedup can be obtained if more wavelength clusters are used for the machines used here, occurs at about 5 to 8 clusters. More clusters will not lead to larger speedups, as expected. Larger speedups

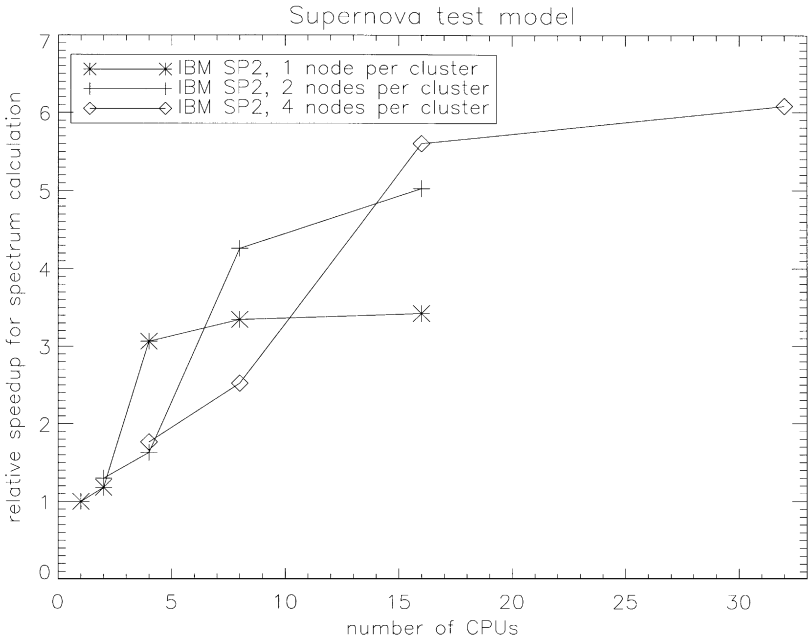

Fig. 4. Scalability of the Supernova model atmosphere test run as function of the number of nodes (processing elements or nodes) used. The y-axis gives the speedup obtained relative to the serial run. The different symbols show the results for different numbers of worker tasks for each wavelength cluster.

can be obtained by using more worker nodes per cluster, which also drastically reduces the amount of memory required on each node.

4. Discussion and conclusions

We have presented our approach to the numerical solution to the generalized stellar atmosphere problem in the presence of rapidly expanding flows. We have shown how the use of accelerated Λ operators may result in the formulation of the problem in such a way that extremely detailed model atoms may be handled in NLTE and the problem can be parallelized in a way that significantly reduces the per processor memory and CPU requirements with modest communication overhead. Parallelization also allows much more complex models to be calculated by giving us access to the large memory sizes that are available on modern parallel supercomputers. Currently, our largest model calculations involve 6000 atomic NLTE level with 65000 primary NLTE lines that are modeled individually, 2–10 million weak atomic secondary NLTE and LTE background lines and, for models of cool stellar winds, 150 million molecular lines. Simulations of this size and level of detail were simply not possible before the development of new radiative transfer algorithms and the availability of parallel supercomputers. We believe that the next step — the computation of moving flows in three spatial dimensions, is becoming tractable on modern parallel supercomputers. There continues to be an urgent need for improvements in the fundamental atomic data which serves as input to these calculations.

Acknowledgements

We thank our many collaborators who have contributed to the development of PHOENIX, in particular we would like to thank France Allard, David Branch, Steve Shore, Sumner Starrfield, Jason Aufdenberg, and Andreas Schweitzer. This work was supported in part by NASA ATP grant NAG 5-3018 and LTSA grant NAG 5-3619 and NSF grant AST-9720804 to the University of Georgia, and by NSF grant AST-9417242, NASA grant NAG5-3505 and an IBM SUR grant to the University of Oklahoma. Some of the calculations presented in this paper were performed on the IBM SP2 and SGI Origin 2000 of the UGA UCNS, at the San Diego Supercomputer Center (SDSC), the Cornell Theory Center (CTC), and at the National Center for Supercomputing Applications (NCSA), with support from the National Science Foundation, and at the NERSC with support from the DoE. We thank all these institutions for a generous allocation of computer time.

References

[1] F. Allard, P.H. Hauschildt, Astrophys. J. 445 (1995) 433.
[2] L.H. Auer, D.V. Blerkom, Astrophys. J. 178 (1972) 175.
[3] L. Auer, in: L.Crivellari, I. Hubeny, D.G. Hummer (Eds.), Stellar Atmospheres: Beyond Classical Models, NATO ASI Series, Kluwer, Dordrecht, 1991, p. 9.
[4] E. Baron, P.H. Hauschildt, Parallel implementation of the PHOENIX generalized stellar atmosphere program. II: wavelength parallelization, Astrophys. J. 495 (1998) 370.
[5] E. Baron, P.H. Hauschildt, P. Nugent, D. Branch, MNRAS 283 (1996) 297.
[6] C.J. Cannon, JQSRT 13 (1973) 627.
[7] L.J. Caroff, P.D. Noerdlinger, J.D. Scargle, Astrophys. J. 176 (1972) 439.
[8] J.I. Castor, MNRAS 149 (1970) 111.
[9] G.H. Golub, C.V. Loan, Matrix Computations, The Johns Hopkins University Press, Baltimore, MD, 1989.
[10] W.-R. Hamann, in: Kalkofen [20] p. 35.
[11] P.H. Hauschildt, JQSRT 47 (1992) 433.
[12] P.H. Hauschildt, JQSRT 50 (1993) 301.
[13] P.H. Hauschildt, E. Baron, JQSRT 54 (1995) 987.
[14] P.H. Hauschildt, E. Baron, F. Allard, Astrophys. J. 483 (1997) 390.
[15] P.H. Hauschildt, E. Baron, S. Starrfield, F. Allard, Astrophys. J. 462 (1996) 386.
[16] P.H. Hauschildt, M. Best, R. Wehrse, Astron. Astrophys. 247 (1991) L21.
[17] P.H. Hauschildt, S. Starrfield, S.N. Shore, F. Allard, E. Baron, Astrophys. J. 447 (1995) 829.
[18] P.H. Hauschildt, H. Störzer, E. Baron, JQSRT 51 (1994) 875.
[19] P.H. Hauschildt, R. Wehrse, JQSRT 46 (1991) 81.
[20] W. Kalkofen (Ed.), Methods in Radiative Transfer, Cambridge Univ. Press, Cambridge, 1987.
[21] C. Magnan, JQSRT 10 (1970) 1.
[22] Message Passing Interface Forum. MPI: A Message-Passing Interface Standard, Version 1.1, Univ. of Tennessee, Knoxville, TN, 1995.
[23] D. Mihalas, Stellar Atmospheres, 1st edn., W.H. Freeman, New York, 1970.
[24] D. Mihalas, Stellar Atmospheres, 2nd edn., W.H. Freeman, New York, 1978.
[25] D. Mihalas, Astrophys. J. 237 (1980) 574.
[26] D. Mihalas, P. Kunasz, D. Hummer, Astrophys. J. 202 (1975) 465.
[27] D. Mihalas, B.W. Mihalas, Foundations of Radiation Hydrodynamics, Oxford University, Oxford, 1984.
[28] K.C. Ng, J. Chem. Phys. 61 (1974) 2680.
[29] G.L. Olson, L.H. Auer, J.R. Buchler, JQSRT 38 (1987) 431.

[30] G.L. Olson, P.B. Kunasz, JQSRT 38 (1987) 325.
[31] G.B. Rybicki, D.G. Hummer, Astron. Astrophys. 245 (1991) 171.
[32] G.B. Scharmer, in: W. Kalkofen (Ed.), Methods in Radiative Transfer, Cambridge Univ. Press, Cambridge, 1984, p. 173.
[33] S. Turek, preprint, 1993.
[34] A. Unsöld, Physik der Sternatmosphären, 2nd edn., Springer, Heidelberg, 1968.
[35] P.W. Vinsome, in: Proceedings of the 4th Symposium on Reservoir Simulation. Soc. of Petroleum Engineers, 1976, p. 149.
[36] K. Werner, in: Kalkofen [20] p. 67.